STARS

University of Central Florida
STARS

Faculty Bibliography 2010s | Faculty Bibliography

1-1-2010

Directed assembly of solution processed single-walled carbon nanotubes via dielectrophoresis: From aligned array to individual nanotube devices

Paul Stokes
University of Central Florida

Saiful I. Khondaker
University of Central Florida

Find similar works at: https://stars.library.ucf.edu/facultybib2010
University of Central Florida Libraries http://library.ucf.edu

This Article is brought to you for free and open access by the Faculty Bibliography at STARS. It has been accepted for inclusion in Faculty Bibliography 2010s by an authorized administrator of STARS. For more information, please contact STARS@ucf.edu.

Recommended Citation

Stokes, Paul and Khondaker, Saiful I., "Directed assembly of solution processed single-walled carbon nanotubes via dielectrophoresis: From aligned array to individual nanotube devices" (2010). *Faculty Bibliography 2010s*. 828.
https://stars.library.ucf.edu/facultybib2010/828

Directed assembly of solution processed single-walled carbon nanotubes via dielectrophoresis: From aligned array to individual nanotube devices

Paul Stokes, and Saiful I. Khondaker

Citation: Journal of Vacuum Science & Technology B **28**, C6B7 (2010); doi: 10.1116/1.3501347
View online: https://doi.org/10.1116/1.3501347
View Table of Contents: https://avs.scitation.org/toc/jvb/28/6
Published by the American Vacuum Society

ARTICLES YOU MAY BE INTERESTED IN

High quality solution processed carbon nanotube transistors assembled by dielectrophoresis
Applied Physics Letters **96**, 083110 (2010); https://doi.org/10.1063/1.3327521

Solution processed large area field effect transistors from dielectrophoreticly aligned arrays of carbon nanotubes
Applied Physics Letters **94**, 113104 (2009); https://doi.org/10.1063/1.3100197

Single- and multi-wall carbon nanotube field-effect transistors
Applied Physics Letters **73**, 2447 (1998); https://doi.org/10.1063/1.122477

Low voltage, high performance inkjet printed carbon nanotube transistors with solution processed ZrO_2 gate insulator
Applied Physics Letters **103**, 082119 (2013); https://doi.org/10.1063/1.4819465

The work function of the elements and its periodicity
Journal of Applied Physics **48**, 4729 (1977); https://doi.org/10.1063/1.323539

Well-aligned and suspended single-walled carbon nanotube film: Directed self-assembly, patterning, and characterization
Applied Physics Letters **94**, 261903 (2009); https://doi.org/10.1063/1.3151850

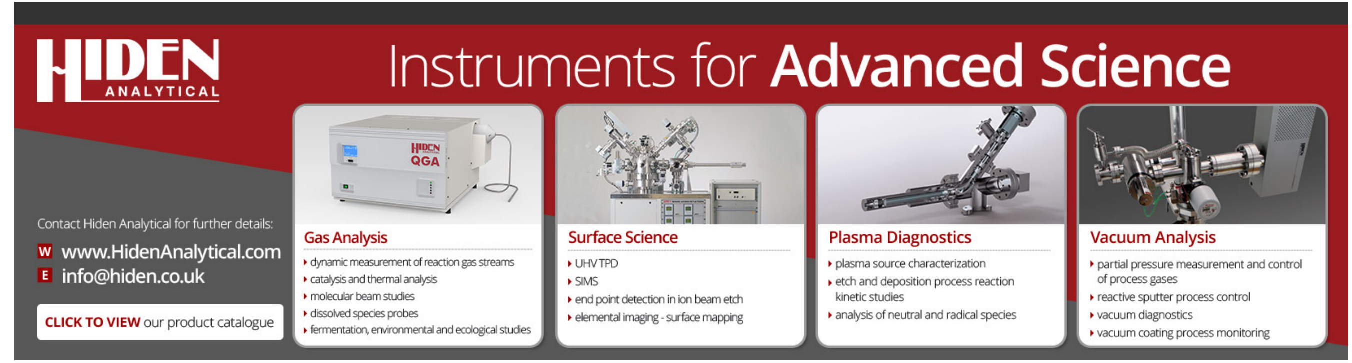

Directed assembly of solution processed single-walled carbon nanotubes via dielectrophoresis: From aligned array to individual nanotube devices

Paul Stokes and Saiful I. Khondaker[a)]
Nanoscience Technology Center and Department of Physics, University of Central Florida, 12424 Research Parkway, Orlando, Florida 32826

(Received 9 July 2010; accepted 7 September 2010; published 29 November 2010)

The authors demonstrate directed assembly of high quality solution processed single-walled carbon nanotube (SWNT) devices via ac dielectrophoresis using commercially available SWNT solutions. By controlling the shape of the electrodes, concentration of the solution, and assembly time, the authors are able to control the assembly of SWNTs from dense arrays down to individual SWNT devices. Electronic transport studies of individual SWNT devices show field effect mobilities of up to 1380 $cm^2/V\ s$ for semiconducting SWNTs and saturation currents of up to $\sim 15\ \mu A$ for metallic SWNTs. The field effect mobilities are more than an order of magnitude improvement over previous solution processed individual SWNT devices and close to the theoretical limit. Field effect transistors (FET) fabricated from aligned two-dimensional arrays of SWNT show field effect mobility as high as 123 $cm^2/V\ s$, which is three orders of magnitude higher than the solution processed organic FET devices. This study shows promise for commercially available SWNT solution for the parallel fabrication of high quality nanoelectronic devices. © *2010 American Vacuum Society.* [DOI: 10.1116/1.3501347]

I. INTRODUCTION

The unique electronic properties of single-walled carbon nanotubes (SWNTs) make them promising candidates for future nanoelectronic devices.[1] For practical applications in nanoelectronics, it is important that SWNTs are assembled at selected positions of the circuit with high yield. Chemical vapor deposition (CVD) growth of SWNTs using lithographically patterned catalytic islands and then making electrical contact to them has been used for the parallel fabrication of SWNT devices.[2,3] Although CVD grown SWNT has shown good device properties, high growth temperature (900 °C) is a major bottleneck to make them compatible with current complementary metal-oxide-semiconductor (CMOS) fabrication technologies.

An attractive alternative to CVD growth techniques for the high throughput assembly of SWNT electronic devices at selected positions of the circuit is from postsynthesis fabrication using solution processed SWNTs.[4] Solution processing could be advantageous due to its ease of processing at room temperature, CMOS compatibility, and potential for scaled up manufacturing of SWNT devices on various substrates. Several assembly techniques from solution include chemical and biological patterning,[5,6] flow assisted alignment,[7] Langmuir–Blodgett assembly,[8] bubble blown films,[9] contact printing,[10] spin coating assisted alignment,[11] and evaporation driven self-assembly.[12] However, most of these techniques are used either for only large area devices or only single nanotube devices. In addition, most of these assembly techniques require postetching to remove excess SWNTs in the circuit.

Dielectrophoresis (DEP) offers a convenient way in which SWNTs can be precisely positioned from solution at room temperature using a nonuniform ac electric field on prepatterned electrodes.[13–24] DEP can be advantageous over other solution processed techniques because it allows for the positioning from large areas to individual SWNTs at predefined coordinates of the circuit and does not require the need of postetching or transfer printing. One crucial aspect of the DEP process is the quality of the SWNT solution. The solution should be free of catalytic particles, contain mostly individual SWNTs, and be stable for long periods of time. Catalytic particles in the solution tend to make their way into the electrode gap with the SWNTs during assembly process due to their highly conducive nature which can disrupt their device performance. Solutions containing bundles make it difficult to only obtain individual SWNTs reproducibly into the electrode gap as the DEP force will likely select the larger bundles due to their higher dielectric constant and conductivity. Additionally, avoiding degradation of the SWNTs from processing is extremely important to maintain their excellent electrical properties.[25]

In this article, we used a clean commercially available, surfactant-free SWNT solution combined with the DEP technique to achieve directed assembly of high quality SWNT devices with high yield. By optimizing the device design, concentration of the solution, and assembly time, we are able to control the assembly of SWNTs from large scale arrays down to individual devices. Comparison of the assembly from commercial solution of SWNT with other homemade solutions in common organic solvents show that the clean

[a)]Author to whom correspondence should be addressed; electronic mail: saiful@mail.ucf.edu

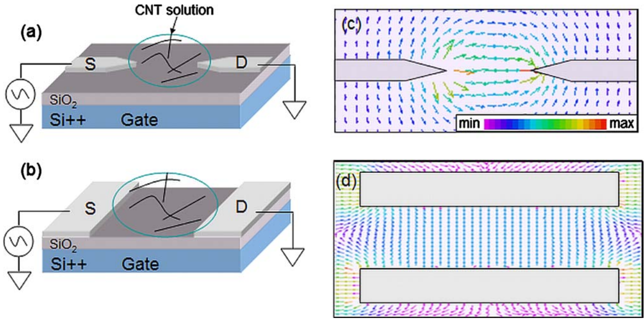

FIG. 1. (Color online) (a) Cartoon of the electrode patterns for DEP assembly of (a) individual SWNTs and (b) 2D arrays of SWNTs. 2D simulated electric field around the electrode gap for (c) the taper shaped electrodes and (d) parallel plate electrodes.

assembly was obtained from the commercial solution. Electronic transport properties of individual semiconducting SWNTs show field effect mobilities up to 1380 cm^2/V s and saturation currents up to ~ 15 μA for metallic SWNTs. The field effect mobilities are more than an order of magnitude improvement over previous solution processed individual SWNT devices and close to the theoretical limit. Additionally, field effect transistors (FET) fabricated from aligned two-dimensional (2D) arrays of SWNT show field effect mobilities as high as 123 cm^2/V s, which is three orders of magnitude higher than solution processed organic FET devices.

II. EXPERIMENTAL DETAILS

A. Electrode design and fabrication

Devices were fabricated on heavily doped silicon substrates capped with a thermally grown 250 nm thick SiO_2 layer. The electrode patterns were fabricated by a combination of optical and electron beam lithography (EBL). First, contact pads and electron beam markers were fabricated with optical lithography using double layer resists (LOR 3A/ Shipley 1813) developing in CD26, thermal evaporation of 3 nm Cr and 50 nm Au followed by lift-off. Smaller electrode patterns were fabricated with EBL using single layer PMMA resists and then developing in (1:3) methyl isobutyl ketone:isopropal alchohol (MIBK:IPA). After defining the patterns, 2 nm Cr and 25 nm thick Pd were deposited using electron beam deposition followed by lift-off in warm acetone. Pd was used because it is known to make the best electrical contact to SWNTs.[3] Figures 1(a) and 1(b) show a cartoon of the electrode patterns for the DEP assembly of individual SWNTs and parallel arrays of SWNTs, respectively. The electrode patterns for the alignment of individual tubes use a pair of adjacent taper shaped electrodes with sharp tips separated by 1 μm, whereas the electrode patters for aligned arrays of SWNTs were done using 200 μm long parallel electrodes with 5 μm spacing.

B. Solution preparation

We used three different SWNT solutions for the DEP assembly: (i) A homemade dimethylformamide (DFM) solution, (ii) homemade dichloroethane (DCE) solution, and (iii) already suspended, surfactant-free aqueous SWNT solution purchased from Brewer Science Inc.[26] The DMF-SWNT suspension was made by ultrasonically dispersing HiPCO grown SWNTs (Carbon Nanotechnologies Inc.) in ~ 5 ml DMF and 1 ml trifluoroacetic acid (TFA). TFA was used to dissolve any unwanted catalytic particles and amorphous carbon from the bulk material. After dissolving the SWNTs in DMF/TFA, the solution was centrifuged, the supernatant was decanted, and the solid is then redispersed for further dispersion/centrifugation/decantation cycles. The final solution was diluted until it became clear and then sonicated for several minutes before assembly. The DCE mixture was made by simply adding a very small pinch of the HiPCO SWNT soot to ~ 4 ml of DCE and then sonicating for $\sim 5-10$ min before the assembly. The commercial solution has an original SWNT concentration of ~ 50 $\mu g/ml$ and was diluted using de-ionized (DI) water to a desired concentration.

C. Dielectrophoretic assembly

The directed assembly of SWNTs at predefined electrode positions was done in a probe station under ambient conditions. A small drop of SWNT solution was cast onto the chip containing the electrode pairs. An ac voltage of 1 MHz, 5 $V_{p\text{-}p}$ was applied using a function generator between the source and drain electrodes or by a simultaneous deposition technique[14,22] (between source and gate) to align at several electrode pairs simultaneously. The ac voltage gives rise to a time averaged dielectrophoretic force. For an elongated object, it is given by $F_{DEP} \propto \varepsilon_m \, \mathrm{Re}[K_f] \nabla E^2_{\mathrm{rms}}$, $K_f = (\varepsilon^*_p - \varepsilon^*_m)/\varepsilon^*_m$, and $\varepsilon^*_{p,m} = \varepsilon_{p,m} - i(\sigma_{p,m}/\omega)$, where ε_p and ε_m are the permittivities of the nanotube and, solvent respectively, K_f is the Claussius–Mossotti factor, σ is the conductivity, and $\omega = 2\pi f$ is the frequency of the applied ac voltage.[27] The induced dipole moment of the nanotube interacting with the strong electric field causes the nanotubes to move in a translational motion along the electric field gradient.

Figures 1(c) and 1(d) show a simulation of the electric field around the electrode gap for the adjacent taper shaped electrode and parallel plate electrode, respectively. The simulations were done using a commercially available software (FLEX PDE) assuming that the potential phasor is real and therefore using the electrostatic form of the Laplace equation ($\nabla^2 \Phi = 0$).[14] Hence we can set the effective potential of the electrodes to $\Phi = \pm V_{p\text{-}p}/2$ for our simulation. From Fig. 1(c), it can be seen that the strongest electric field lines are confined at the sharp tips. This increases the probability of aligning individual SWNTs. For the parallel plate geometry, the electric field is uniform throughout the electrode gap allowing for many nanotubes to align parallel to one another throughout the gap. After the assembly, the function genera-

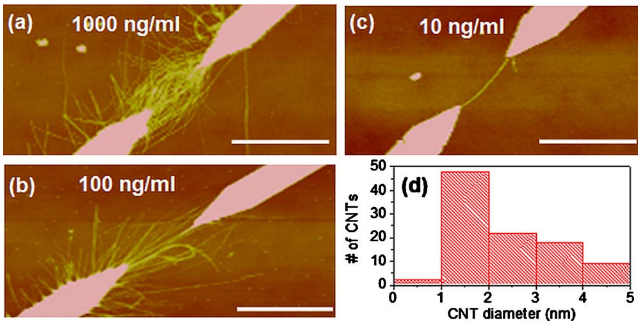

FIG. 2. (Color online) AFM image of nanotubes assembled between the electrodes with SWNT concentrations of (a) 1000 ng/ml (b) 100 ng/ml, and (c) 10 ng/ml in the solution. Scale bar: 1 μm in all images. (d) Histogram of diameters for over 100 nanotube devices.

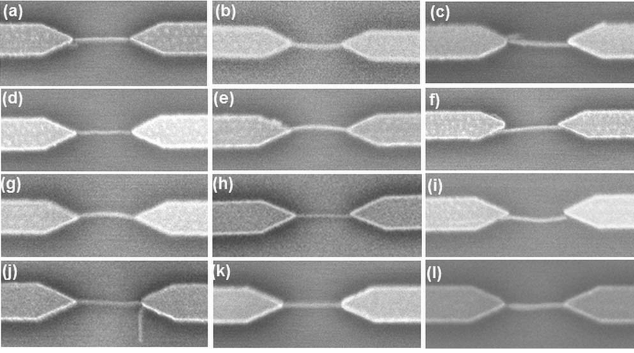

FIG. 3. [(a)-(l)] SEMs of several individual SWNT assembled via DEP from commercial solution at a concentration of ~10 ng/ml. Gap between the electrodes is 1 μm.

tor was turned off and the sample was blown dry by a stream of nitrogen gas.

III. RESULTS AND DISCUSSIONS

A. Controlling the assembly of individual SWNTs

Figure 2 shows the effect of SWNT concentration on the DEP assembly using the commercial solution diluted in DI water. We use a simultaneous deposition technique[14,22] in this case, applying the ac field between source and gate for 3 min. Figure 2(a) shows an atomic force microscopy (AFM) image of a device after the assembly for a SWNT concentration of 1000 ng/ml. Dilution of the solution by ten times to 100 ng/ml concentration yield less SWNTs in the gap, as shown in Fig. 2(b). It can be seen here in both cases that the SWNTs mimic the electric field lines around the electrode gap, as simulated in Fig. 1(c). The yield for the 1000 ng/ml and 100 ng/ml concentration is >95%. By diluting the solution to 10 ng/ml, we obtained an individual SWNT in the gap [Fig. 2(c)]. The diameter of this individual SWNT is ~2.0 nm, measured by AFM. Figure 2(d) shows a histogram of ~100 individual SWNTs giving an average diameter of 2.0 ± 0.2 nm. Approximately 10% of the diameters are greater than 3.5 nm, which is an indication of the possible presence of some double-walled nanotubes or large diameter SWNTs.[28] The total yield of individual SWNTs at low concentration is ~20% on average and as high as 35% for a single chip. Figure 3 shows a number of SEM images of individual nanotubes assembled by this technique. It can be seen here that the devices are free of bundles and catalytic particles which stems from the quality of the commercial solution.

B. Comparison of solutions

We investigated the effect of the different solutions at low concentration (~10 ng/ml) on the DEP assembly. In contrast to the commercial solution in water, for the DMF and DCE solutions, we apply the ac voltage between one pair at a time for ~5 s. This is done because long trapping times are more complex to use as DMF and DCE evaporate quickly in air. Figure 4(a) shows a representative AFM image after the assembly for the DMF solution. As can be clearly seen here, the resulting SWNT deposition contains a bundle and catalytic particles shown by the arrows. At certain areas along the SWNT, the diameter is as large as 30–40 nm. Figure 4(b) shows the representative AFM image of a device after assembling the SWNTs using DCE. The resulting device also contains catalytic particles near the electrode tip on the right and shows diameters up to 10 nm along the SWNT. Figure 4(c) shows an AFM image of a device after assembly by using the Brewer Science SWNT solution. It is clear from the AFM image that the SWNT is individual and does not contain any catalytic particles. The commercial solution turned out to be stable for months, therefore increasing the reproducibility. For the DCE solution we were able to assemble ~10 individual SWNT devices out of ~80 tries, however, all of them contained catalytic particles (with diameter > 10 nm) attached to the tubes. Another problem that arises when using DCE is that it evaporates in air very quickly, it is highly toxic, volatile, and did not remain stable for more than a few hours. In the DMF case, the solutions also only remained stable for a short period of time and the results often came with larger diameter bundles >15 nm out of ~50 tries.

As can be concluded here, the commercial solution yielded the best results for the assembly of clean and individual SWNT devices. The good results from the commercial solution are due to several reasons. First, its very low density of impurity particles (less than 50 ppb)[26] is particularly advantageous in the DEP process because catalytic particles in the solution tend to make their way into the electrode gap during DEP due to their high conductivity. This is displayed

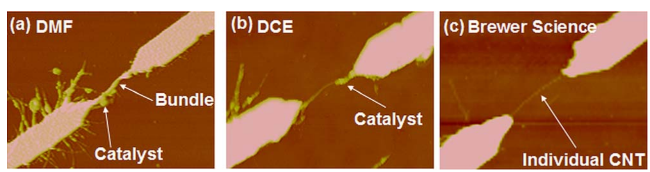

FIG. 4. (Color online) Representative AFM images of SWNTs assembled via DEP (a) from DMF solution, (b) from DCE solution, and (c) the Brewer Science solution.

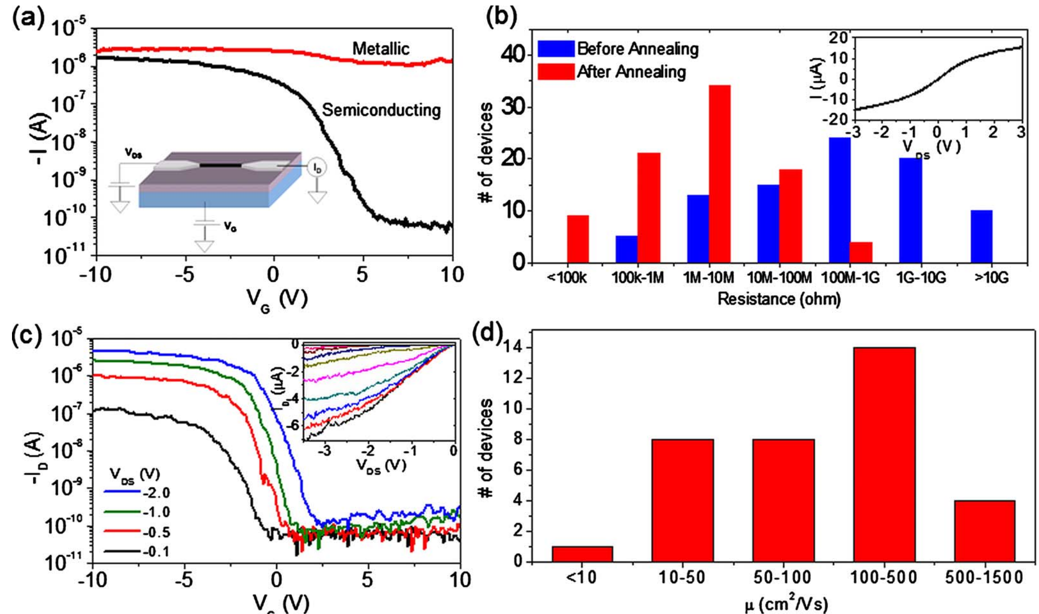

FIG. 5. (Color online) (a) Current vs gate voltage characteristics for semiconducting and metallic devices. $V_{DS}=-0.5$ V Inset: Schematic diagram of device geometry and measurement setup showing a SWNT between source and drain. (b) Histogram of the contact resistance for metallic devices as-assembled (blue) and metallic devices after annealing (red). (c) Transfer characteristics of a representative SWNT FET device ($d\sim 1.7$ nm) at $V_{DS}=-0.1$, -0.5, -1.0, and -2.0 V. Inset: Output characteristics showing currents up to 7 μA in the saturation regime. V_G is changed from -10 to 10 V in steps of 1 V from bottom to top. (d) Histogram of the mobility for semiconducting devices after annealing. The mobility is ~ 200 cm^2/V s on average and the maximum mobility is ~ 1380 cm^2/V s for ~ 35 measured devices.

here with the homemade solutions [Figs. 4(a) and 4(b)]. Second, the commercial solution contains mostly individual SWNTs. Solutions containing bundles makes it difficult to only obtain individual SWNTs reproducibly into the electrode gap as the DEP force will likely select the larger bundles due to their higher dielectric constant and conductivity, which is also displayed here with the homemade solutions. Finally, because the solution was stable over long periods of time, the solution has a constant and uniform concentration and therefore allows for reproducible results. The stability of the solution is due to the rigorous removal of impurities and from a covalent functionalization of the SWNT surfaces that allow the SWNTs to repel each other in the solution.[26] Therefore, although the DMF and DCE solutions may be optimized for further control, however, due to the reproducible and clean device assembly from the stable commercial solution, we only continued further investigation of the devices stemming from the commercial solution.

C. Electrical transport properties of individual nanotube devices

After the DEP assembly, the room temperature dc electrical transport measurements of the devices were done in a probe station using a DL instruments 1211 current preamplifier combined with a high resolution DAC card interfaced with LABVIEW. The inset of Fig. 5(a) shows a cartoon of the measurement setup where we use the highly doped Si as a back gate. After two terminal resistance measurements of the as-assembled devices, they were annealed in a tube furnace using ultrahigh purity Ar/H_2 (1:10 ratio/$Ar:H_2$) at 200 °C for 1 h. During cool down, the gas was left flowing until the sample reached room temperature. We measured a total of 120 individual SWNT devices. Figure 5(a) shows the drain current (I_D) as a function of back gate voltage (V_{BG}) of a representative metallic and a semiconducting device for a fixed source-drain voltage (V_{DS}) of -0.5 V. The metallic nanotubes show weak modulation in I_D as a function of V_{BG}, whereas semiconducting nanotubes show several orders of magnitude change in I_D as a function of V_{BG}. Approximately 70% of our devices show metallic or semimetallic behavior with current on-off ratio (I_{on}/I_{off}) less than 10, and 30% of the devices show semiconducting behavior with on-off ratios >10. The higher percentage of metallic nanotubes during the assembly is expected since, to the first order approximation, DEP tends to attract metallic SWNTs over semiconducting SWNTs because metallic SWNTs have a higher dielectric constant. However, several recent experimental and theoretical studies show that both metallic and semiconducting SWNT can be assembled using DEP due to other contributing forces such as electrothermal flow, fluid flow, and Brownian motion.[29,30]

1. Metallic nanotube device properties

Figure 5(b) is a histogram of the contact resistance for the metallic SWNT devices before annealing and after annealing. From here it can be seen that the contact resistance is reduced by two to three orders of magnitude on average due to annealing. The average contact resistances before and after annealing are 100 MΩ and 1 MΩ, respectively. The contact resistance is as low as ~ 25 kΩ after annealing for

certain devices. To characterize the quality of the metallic SWNTs and their contact, we measured the I_D-V_{DS} characteristics at high bias after annealing. The inset of Fig. 5(b) shows a plot of I_D versus V_{DS} (up to 3 V) for a low contact resistance device that gives a saturation current of $\sim 15\ \mu$A at high bias. This is similar to a 1 μm long individual metallic SWNT with Ohmic contacts grown by the CVD method,[31] demonstrating a high quality contact can be achieved from DEP assembled metallic devices.

2. Semiconducting nanotube device properties

Figure 5(c) shows the transfer characteristics, I_D-V_G, for a representative FET device at $V_{DS}=-0.1$, -0.5, -1.0, and -2.0 V ($d\sim 1.7$ nm) showing *p*-type transport characteristics. The drain current changes by several orders of magnitude with gate voltage and maintains approximately the same off-current for each V_{DS}. For example, at $V_{DS}=-1.0$ V, the on-off ratio is $\sim 3.6\times 10^4$ ($I_{\text{off}}\sim -70$ pA and $I_{\text{on}}\sim -2.5\ \mu$A). The linear conductance in the on-state ($G_{\text{on}}=I_{\text{on}}/V_{DS}$) is $\sim 2.5\ \mu$S at $V_{DS}=-1.0$ V. In the inset of Fig. 5(c), we plot I_{DS} versus V_{DS} up to the saturation regime at different gate voltages (from -10 to 10 V, bottom to top). Output currents are as high as 7 μA, comparable to Pd contacted CVD SWNTs of similar diameter, directly grown on the substrate.[28]

The field effect mobility was calculated from the linear regime in Fig. 5(c) from $\mu=(L^2/C_G\cdot V_{DS})(dI_D/dV_G)$, where the gate capacitance is $C_G=2\pi\varepsilon L/\ln(2h/r)$, L is the length of the channel, $\varepsilon=3.9\varepsilon_0$ is the dielectric constant for SiO_2, h is the thickness of the oxide, and r is the radius of the SWNT,[32] and $dI_D/dV_G=g_m$ is the transconductance. We find $g_m\sim 0.57\ \mu$S at $V_{DS}=-1.0$ V and setting $r=0.85$ nm gives a mobility of $\mu\sim 163\ \text{cm}^2/\text{V s}$.

Figure 5(d) shows a histogram of the mobility for all 35 semiconducting devices. We obtain a median mobility $\sim 200\ \text{cm}^2/\text{V s}$ and a maximum mobility $\sim 1380\ \text{cm}^2/\text{V s}$. For our highest mobility device, we can compare with the theoretical limit at room temperature for clean SWNTs,[32,33] $\mu_{\text{peak}}\sim 1000\ \text{cm}^2/\text{V s}\times(d(\text{nm}))^2$, where d is the diameter of the tube, we find $\mu_{peak}\sim 1700\ \text{cm}^2/\text{V s}$, which is reasonably close to the experimental value indicating that this device is being pushed close to it's performance limit. The maximum mobility is ~ 20 times higher than the highest previous reported values for other solution processed devices and close to what is expected in high quality direct growth CVD devices of similar diameter. We speculate that the improved device performance stems from the nonexistence of residual surfactant and the cleanliness of the as-assembled devices with the absence of bundles.

D. Large area assembly and device properties

Large scale parallel arrays of SWNTs are of considerable interests in order to increase device to device homogeneity and their expected higher performance compared to organic electronic FETs.[34] In addition, aligned arrays offer added advantage compared to random thin film as the transport through SWNT-SWNT interconnects can be minimized. We used diluted commercial solution ($\sim 1\ \mu$g/ml) for this assembly along with parallel electrode. Figure 6(a) shows a SEM image for a part of device after the assembly. The density of the aligned array is ~ 1 SWNT/μm on average giving ~ 200 SWNTs total in the channel. After the assembly, an additional Pd top contact (not shown here) was fabricated to reduce the overall contact resistance.

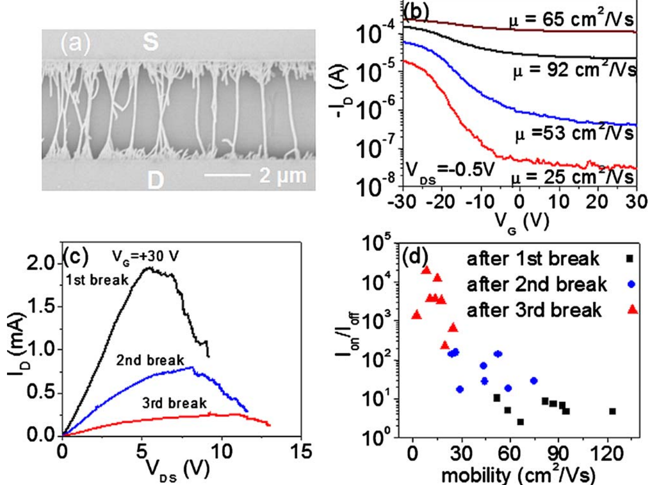

FIG. 6. (Color online) (a) SEM image of a part of a SWNT aligned array device. (b) I_D vs back gate voltage V_G at constant V_{DS} of -0.5 V after successive electrical breakdown. (c) A representative plot of drain current (I_D) vs source-drain voltage (V_{DS}) for three sequential breakdowns (first, second, and third break) (d) Plot of on-off ratios and corresponding mobility for several measured devices after each breakdown.

The two terminal resistance was typically in the range 2–5 kΩ. The array contains a mixture of metallic and semiconducting SWNTs as evident in the I-V_G for the as-assembled device [Fig. 6(b) top curve] where the device shows semimetallic behavior with an on-off ratio of ~ 3. To increase the on-off ratio, we performed an electrical breakdown procedure to controllably reduce the metallic pathways.[35] Figure 6(c) shows a plot of I_D versus V_{DS} for three sequential breakdowns (first, second, and third breaks). The back gate was held constant at $V_G=+30$ V to deplete the carriers in the *p*-type semiconducting SWNTs, while we ramped up V_{DS} to eliminate the metallic SWNTs. As V_{DS} is ramped up, the SWNTs start to breakdown and I_D begins to fall. In order to obtain reproducible results, each breakdown is stopped when I_D is about 50% of its peak value at which point V_{DS} is swept back to zero. When the third breakdown reaches $\sim 50\%$ of its peak value, I_D can range from ~ 0.03 to 0.12 mA.

Figure 6(b) shows I_D versus V_G characteristics for a typical device after each breakdown. The uppermost curve was the initial sweep showing a mobility of 65 $\text{cm}^2/\text{V s}$ with very little on-off ratio. The device mobility was calculated using the formula $\mu=(LA/WV_{DS}C)/(dI_D/dV_G)$. The capacitance C of the SWNT FET array device was approximated from

$$C=\frac{A\cdot D}{\left[C_Q^{-1}+\frac{1}{2\pi\varepsilon}\ln\left[\frac{\sinh(2\pi t_{ox}D)}{\pi RD}\right]\right]},$$

where $C_Q=4\times10^{-10}$ F/m is the quantum capacitance, R is the radius of the nanotubes, and D is the linear density in SWNTs per micrometer of the array.[36]

After the first breakdown, the field effect behavior of the device is enhanced—both the mobility and on-off ratios are increased to 92 $cm^2/V\,s$ and ~6.6, respectively, due to a reduction of metallic pathways. After the second breakdown, the mobility reduces a small amount to 53 $cm^2/V\,s$ and the on-off ratio increases to ~14. Finally, after the third breakdown, the mobility is reduced to 25 $cm^2/V\,s$; however, the on-off ratio increases to ~650.

Figure 6(d) shows the on-off ratio and the corresponding mobility value for several devices after each breakdown. The devices yield median mobility values of 77, 41, and 15 $cm^2/V\,s$ after the three breakdowns, respectively. The highest mobility obtained from all the devices is 123 $cm^2/V\,s$. The mobility values reported here are up to three orders of magnitude higher than typical FET devices made from solution processed polymers.[37]

IV. CONCLUSIONS

We demonstrated directed assembly of high quality solution processed carbon nanotube devices via ac dielectrophoresis using commercially available SWNT solutions. By optimizing the device design, concentration of the solution, and assembly time, we are able to control the assembly of SWNTs from dense arrays to clean individual devices. Electronic transport measurements of individual SWNT revealed mobilities more than an order of magnitude improvement over previous solution processed individual SWNT devices and close to the theoretical limit. FETs fabricated from aligned 2D arrays of SWNT show high field effect mobility, up to three orders of magnitude higher than solution processed organic FET devices. This study shows promise for commercially available SWNT solution for the parallel fabrication of high quality nanoelectronic devices.

ACKNOWLEDGMENT

This work is supported by the U.S. National Science Foundation under Grant No. ECCS-0748091 (CAREER).

[1] P. Avouris, Z. H. Chen, and V. Perebeinos, Nat. Nanotechnol. **2**, 605 (2007).
[2] A. Javey, Q. Wang, A. Ural, Y. Li, and H. Dai, Nano Lett. **2**, 929 (2002).
[3] A. Javey, J. Guo, Q. Wang, M. Lundstrom, and H. Dai, Nature (London) **424**, 654 (2003).
[4] L. Huang, Z. Jia, and S. O'Brien, J. Mater. Chem. **17**, 3863 (2007).
[5] S. Auvray, V. Derycke, M. Goffman, A. Filoramo, O. Jost, and J.-P. Bourgoin, Nano Lett. **5**, 451 (2005).
[6] K. Keren, R. S. Berman, E. Buchstab, U. Sivan, and E. Braun, Science **302**, 1380 (2003).
[7] S. Jin, D. Whang, M. C. McAlpine, R. S. Friedman, Y. Wu, and C. M. Lieber, Nano Lett. **4**, 915 (2004).
[8] Y. Guihua, C. Anyuan, and C. M. Lieber, Nat. Nanotechnol. **2**, 372 (2007).
[9] A. Javey, S. W. Nam, E. S. Friedman, H. Yan, and C. M. Lieber, Nano Lett. **7**, 773 (2007).
[10] K. Kordás *et al.*, Small **2**, 1021 (2006).
[11] M. C. LeMieux, M. Roberts, S. Barman, Y. W. Jin, J. M. Kim, and Z. Bao, Science **321**, 101 (2008).
[12] M. Engel, J. P. Small, M. Steiner, M. Freitag, A. A. Green, M. C. Hersam, and P. Avouris, ACS Nano **2**, 2445 (2008).
[13] K. Yamamoto, S. Akita, and Y. Nakayama, Jpn. J. Appl. Phys., Part 1 **31**, L34 (1998).
[14] A. Vijayaraghavan, S. Blatt, D. Weissenberger, M. Oron-Carl, F. Hennrich, D. Gerthsen, H. Hahn, and R. Krupke, Nano Lett. **7**, 1556 (2007).
[15] B. R. Burg, J. Schneider, M. Muoth, L. Durrer, T. Helbling, N. C. Schirmer, T. Schwamb, C. Hierold, and D. Poulikakos, Langmuir **25**, 7778 (2009).
[16] Z. Zhang, X. Liu, E. E. B. Campbell, and S. Zhang, J. Appl. Phys. **98**, 056103 (2005).
[17] L. F. Dong, V. Chirayos, J. Bush, J. Jiao, V. M. Dubin, R. V. Chebian, Y. Ono, J. F. Conley, Jr., and B. D. Ulrich, J. Phys. Chem. B **109**, 13148 (2005).
[18] S. Banerjee, B. White, L. Huang, B. J. Rego S. O'Brien, and I. P. Herman, Appl. Phys. A: Mater. Sci. Process. **86**, 415 (2007).
[19] P. Makaram, S. Selvarasah, X. Xiong, C.-L. Chen, A. Busnaina, N. Khanduja, and M. R. Dokmeci, Nanotechnology **18**, 395204 (2007).
[20] S. Sorgenfrei, I. Meric, S. Banerjee, A. Akey, S. Rosenblatt, I. P. Herman, and K. L. Shepard, Appl. Phys. Lett. **94**, 053105 (2009).
[21] A. H. Monica, S. J. Papadakis, R. Osiander, and M. Paranjape, Nanotechnology **19**, 085303 (2008).
[22] P. Stokes and S. I. Khondaker, Appl. Phys. Lett. **96**, 083110 (2010).
[23] P. Stokes, E. Silbar, Y. M. Zayas, and S. I. Khondaker, Appl. Phys. Lett. **94**, 113104 (2009).
[24] P. Stokes and S. I. Khondaker, Nanotechnology **19**, 175202 (2008).
[25] P. Stokes and S. I. Khondaker, ACS Nano **4**, 2659 (2010).
[26] See http://www.brewerscience.com for more information about the commercially available SWNT solution.
[27] T. B. Jones, *Electromechanics of Particles* (Cambridge University Press, New York, 1995), p. 140.
[28] W. Kim, A. Javey, R. Tu, J. Cao, Q. Wang, and H. Dai, Appl. Phys. Lett. **87**, 173101 (2005).
[29] M. Dimaki and P. Boggild, Nanotechnology **15**, 1095 (2004).
[30] Y. Lin, J. Shiomi, S. Maruyama, and G. Amberg, Phys. Rev. B **76**, 045419 (2007).
[31] J. Y. Park, S. Rosenblatt, Y. Yaish, V. Sazonova, H. Ustunel, S. Braig, T. A. Arias, P. Brouwer, and P. L. McEuen, Nano Lett. **4**, 517 (2004).
[32] M. J. Biercuk, S. Ilani, C. M. Marcus, and P. L. McEuen, Top. Appl. Phys. **111**, 455 (2008).
[33] X. Zhou, J.-Y. Park, S. Huang, J. Liu, and P. L. McEuen, Phys. Rev. Lett. **95**, 146805 (2005).
[34] Q. Cao and J. A. Rogers, Adv. Mater. **20**, 1738 (2008).
[35] P. G. Collins, M. S. Arnold, and Ph. Avouris, Science **292**, 706 (2001).
[36] S. J. Kang, C. Kocabas, T. Ozel, M. Shim, N. Pimparkar, M. A. Alam, S. V. Rotkin, and J. A. Rogers, Nat. Nanotechnol. **2**, 230 (2007).
[37] T. B. Singh and N. S. Sariciftci, Annu. Rev. Mater. Res. **36**, 199 (2006).